



Severe Damage Law on the Ground Surface Induced by High-Strength Mining: A Case Study From the Shendong Coal Field in China

Weitao Yan^{1,2}, Junting Guo¹, Junjie Chen^{2*}, Yi Tan^{2*}, Shaoge Yan² and Yueguan Yan³

¹State Key Laboratory of Groundwater Protection and Utilization by Coal Mining, Beijing, China, ²State Collaborative Innovation Center of Coal Work Safety and Clean-efficiency Utilization, Henan Polytechnic University, Jiaozuo, China, ³College of Geoscience and Surveying Engineering, China University of Mining and Technology (Beijing), Beijing, China

OPEN ACCESS

Edited by:

Wei Liu,
Chongqing University, China

Reviewed by:

R. M. Yuan,
China Earthquake Administration,
China

Qiang Sun,
Xi'an University of Science and
Technology, China

Geng Jiabo,
Jiangxi University of Science and
Technology, China

*Correspondence:

Junjie Chen
chenjj@hpu.edu.cn
Yi Tan
tanyi@hpu.edu.cn

Specialty section:

This article was submitted to
Geohazards and Georisks,
a section of the journal
Frontiers in Earth Science

Received: 02 December 2021

Accepted: 31 March 2022

Published: 29 April 2022

Citation:

Yan W, Guo J, Chen J, Tan Y, Yan S
and Yan Y (2022) Severe Damage Law
on the Ground Surface Induced by
High-Strength Mining: A Case Study
From the Shendong Coal Field
in China.
Front. Earth Sci. 10:827826.
doi: 10.3389/feart.2022.827826

High-strength mining has the characteristics of shallow buried depth, large mining height, and fast mining speed. Under the condition of high-strength mining, the overburden moves violently and the surface damage is serious. It has caused serious ecological security problems in the mining area. In order to solve this problem, it is necessary to adopt the technology of restoration while mining. The key to the effective implementation of this technology is to clarify the real-time distribution law and generation mechanism of surface damage. In this paper, field investigation and the theoretical analysis method are used for related research. The results show that the surface strenuous move duration is long, the strenuous move area is large, and the surface discontinuous deformation is fully developed. With the characteristics of stepped crack lags behind the location of the working face, the stepped crack spacing and periodic weighting interval are equivalent. Through discussion and analysis, it is found that the cause of serious damage is the strata movement mode of high-strength mining in “two zones” mode. Under the “two zones” mode, the roof has easy-to-slip instability, the bedrock is completely broken along the direction of the bedrock breaking angle, and the weak anti-disturbance ability of the loose layer leads to the surface becoming severely damaged. The research results can provide reference for the formulation of follow-up ecological real-time restoration measures in similar mines.

Keywords: severe damage, crack, dynamic distribution, high-strength mining, “two zones” mode

1 INTRODUCTION

China is the largest coal producer and coal consumer in the world. Coal accounted for about 60% of China's primary energy structure in 2019. The mining of a large number of underground coal resources brings about large-scale overburden movement and surface subsidence, which badly disturbs the original ecology and environment, and seriously affects the safe use of buildings, railways, and highways in the subsidence area. A series of economic, ecological, and environmental problems caused by mining have attracted many people's attention (**Figure 1**).

At present, surface ecological restoration technology is mainly used for the treatment of surface ecological damage in the mining area, but it is usually repaired after mining. There are problems such as poor repair timeliness and low repair rate in this repair mode. In order to solve those problems, the

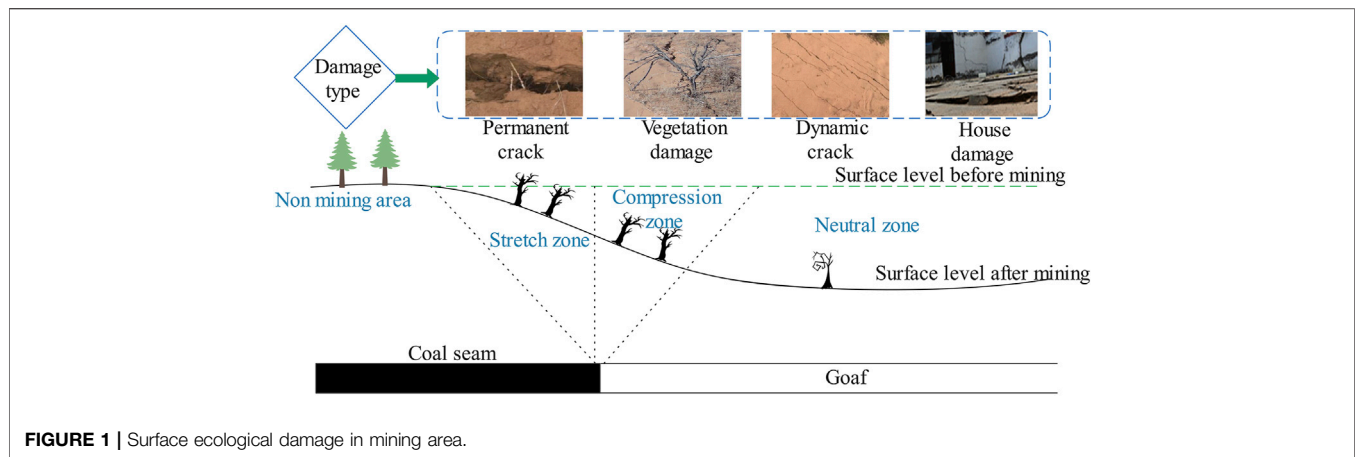


FIGURE 1 | Surface ecological damage in mining area.

technology of “restoration while mining” has been put forward in recent years. This technology emphasizes the timeliness and accuracy of repair, and has good application and promotion. The key to the effective implementation of this technology is to grasp the real-time distribution law of surface damage. This is also the content of this paper.

According to the mining subsidence theory (He et al., 1991; Peng, 1992; National Bureau of Coal Industry, 2017), when the ratio of mining depth to mining height is large and mining velocity is fast, the surface subsidence is generally continuous and regular in time and space. For this continuous surface subsidence, many scholars have undertaken a lot of research on its distribution law (Zhang and Chong, 2012; Cui et al., 2014; Thongprapha et al., 2015; Vervoort, 2016; Yan et al., 2018; Bai et al., 2020), generation mechanism (Wang et al., 1999; Ma et al., 2013; Yu et al., 2015; Suchowska Iwaniec et al., 2016; Salmi et al., 2017; Lian et al., 2020), prediction method (Ren et al., 1989; Ramesh and Ram, 1995; Luo and Cheng, 2009; Yan et al., 2019), and the mining-induced social and ecological problem (Bell et al., 2000; Sinha et al., 2007; Tang, 2009; Saha et al., 2011; Sasaoka et al., 2015). An abundance of research results have been obtained and some important results have been extended to the engineering application. But when the ratio of mining depth to mining height is small and the mining velocity is slow, the surface subsidence will often be accompanied by discontinuous movement, and the surface will often produce tensile cracks, stepped cracks, collapse pits, and other disasters (Fan et al., 2011; Ju and Xu, 2013; Fan et al., 2015; Yan et al., 2018; Chen et al., 2019), which will destroy the soil construction, lower the underground aquifer, reduce agricultural production, and endanger the safety of residents in the subsidence area. This highly destructive mining mode is called high-strength mining. The adverse phenomenon induced by high-strength mining can be divided into two kinds, static and dynamic. The static damage distribution law has been fully studied, and related achievements have been obtained and included in textbooks (He et al., 1991; Peng, 1992). But at present, the research results on the dynamic damage distribution law are still few and insufficient.

Under high-strength mining, the ratio of mining depth to mining height is small, the mining velocity is fast, and the

above-mentioned adverse phenomenon is more serious. To deeply study the dynamic law of severe surface damage induced by high-strength mining, this paper selected working face 22,407 in the Shendong coal field, a typical high-strength mining working face, as the sample. By collecting the relevant information of working face 22,407, we studied the dynamic severe damage distribution law and analyzed its subsidence mechanism.

2 ENGINEERING BACKGROUND OF STUDY AREA

The Halagou coal mine is located in Daliuta Town, Shenmu county, Shaanxi Province, at the junction of Mu Us Desert and Loess Plateau, with an annual output of 10 million tons of coal. Working face 22,407, which belongs to the Halagou coal mine is located in the middle of panel 4. The northwest is the central return air roadway of coal seam 22, the northeast is the designed working face 22,408, the southeast is working face 22,610 designed by the Daliuta coal mine, and the southwest is the goaf of working face 22,406. The ground surface of working face 22,407 has little fluctuation and is covered by aeolian sand. Working face 407 mainly mines coal seam 22.

The coal seam within the mining range of working face 22,407 has a simple structure and is a stable coal seam. The coal seam minability index is 1. The geological structure within the minable range of the working face is simple, without the occurrence of large geological events and the existence of large geological structures.

The working face is mainly affected by the water of the Quaternary loose aquifer. The Quaternary loose aquifer is mainly composed of aeolian sand. The aquifer is 10–24 m thick and has a strong water yield. The normal water inflow of the working face is 75 m³/h.

The size of working face 22,407 is 3224 m × 284 m. The bedrock thickness is 73 m, alluvium thickness is 57 m, and the aquifer thickness is 10–24 m. The average thickness, depth, and dip angle are 5.2 m, 130 m and 1°, respectively. According to the geo-mining conditions and borehole histogram of working face 22,407 (Figure 2), the lithology of the overlying strata in this working face is evaluated as medium hard. The comprehensive

Geological time	Numbers of rock layers	Names of rocks	Thickness (m)	Lithology
Quaternary System	20	Aeolian sand	15.66	
	19	Loess	26.34	
	18	Gritstone	13.47	
Zhiluo Formation	17	Sandy mudstone	4.89	
	16	Siltstone	5.35	
	15	Medium sandstone	6.47	
	14	Fine sandstone	4.57	
	13	Siltstone	4.88	
	12	Medium sandstone	13.98	
Yan'an Formation	11	Siltstone	2.02	
	10	Fine sandstone	6.87	
	9	Fine sandstone	3.64	
	8	Medium sandstone	4.42	
	7	Fine sandstone	5.66	
	6	Sandy mudstone	3.29	
	5	Medium sandstone	2.84	
	4	Siltstone	6.68	
	3	2-2 coal seam	5.39	
	2	Siltstone	5.80	
1	Fine sandstone	4.41		

FIGURE 2 | The borehole log of working face 22407.

mechanized coal mining method is used for mining and the all caving method is used to manage the roof. The average mining velocity of working face 22,407 is 15 m/d.

From the above conditions, we can see that the ratio of mining depth to mining height of working face 22,407 is small and the mining velocity is fast. It is a typical high-strength mining face. Therefore, we chose the data of working face 22,407 to analyze the dynamic damage distribution law and reveal its generation mechanism.

3 MONITORING METHODS AND DATA ACQUISITION

In order to obtain surface movement data, a surface movement observation station was set up on one side of the stoping line of working face 22,407 according to the mine survey regulations. The observation station included one strike surface movement

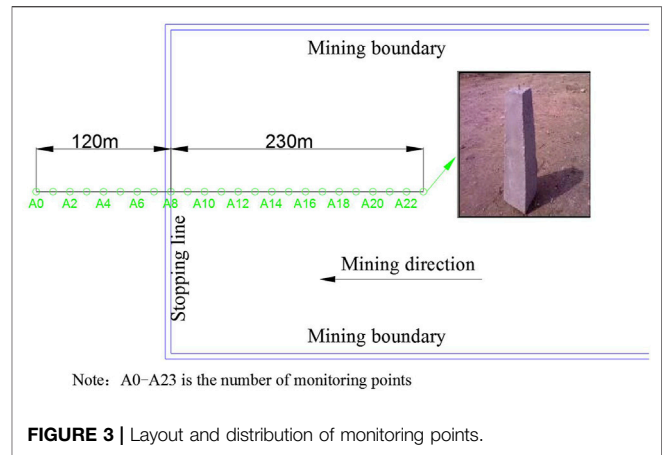


FIGURE 3 | Layout and distribution of monitoring points.

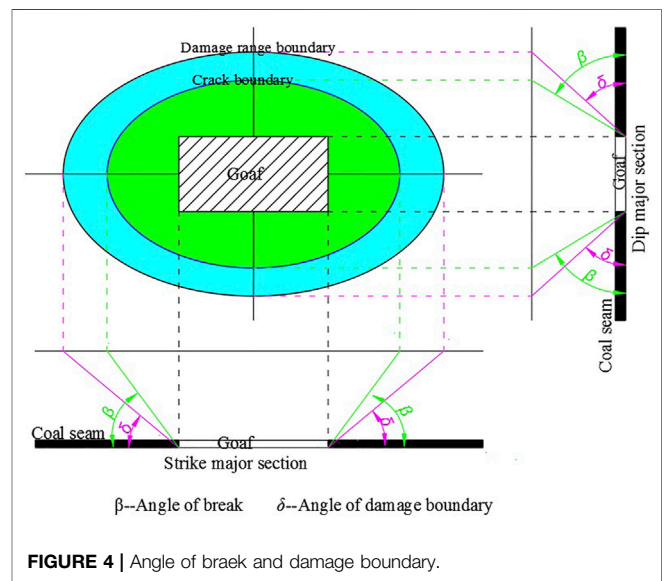


FIGURE 4 | Angle of braek and damage boundary.

observation line. The total length of the strike observation line was 350 m, with 24 monitoring points in total, and the density of monitoring points was 15 m. The point layout is shown in Figure 3.

After the monitoring points were arranged, the following monitoring methods were used for data collection (Table 1).

4 RESULTS

4.1 Surface Damage Range

After the exploitation of underground coal resources, the area of surface mining damage was much larger than that of underground mining. According to the knowledge of mining subsidence, the angle of the damage boundary is often used to characterize the range of ground surface movement, and the angle of break is used to characterize the distribution range of surface damage, as shown in Figure 4.

The angle of the damage boundary value can be calculated with Formula (1).

TABLE 1 | Monitoring items and means.


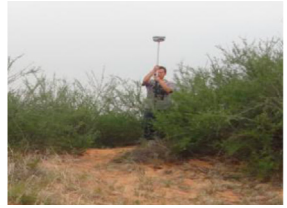
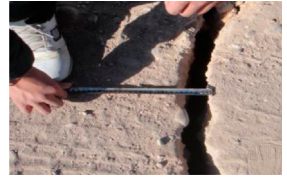
Numbers	Monitoring items	Monitoring means	Corresponding measured photos
1	Subsidence	Leveling	
2	Horizontal displacement	Differential GPS real-time kinematic positioning	
3	Crack	Tape measurement	

TABLE 2 | Duration of each movement period.

	Initial period(d)	Active period(d)	Weakening period(d)
Halagou 22407	9	150	200

$$\beta = \arctan \frac{H}{L_1} \tag{1}$$

Where β is the angle of damage boundary; H is the mining depth; and L_1 is the horizontal distance from the boundary of goaf to the boundary point of 10 mm subsidence. Generally, the value of the boundary angle is approximately 50–60°. The angle of the break value can be calculated with **Formula (2)**.

$$\delta = \arctan \frac{H}{L_2} \tag{2}$$

Where δ is the angle of the break and L_2 is the horizontal distance from the boundary of goaf to the surface critical deformation point. The surface critical deformation point is determined from the outermost point with the inclination of 3 mm/m, curvature of 0.2 mm/m², and horizontal movement of 2 mm/m. Generally, the value of boundary angle is approximately 75°.

The inclination, curvature, and horizontal movement value can be calculated with **Formula (3)**.

$$\begin{aligned} i_{12} &= \frac{w_2 - w_1}{l_{12}} \\ K_{123} &= \frac{i_{23} - i_{12}}{\frac{1}{2}(l_{12} + l_{23})} \\ \epsilon_{12} &= \frac{u_2 - u_1}{l_{12}} \end{aligned} \tag{3}$$

Where w is the subsidence value; i is the inclination value; ϵ is the horizontal movement value; and u is the horizontal displacement value.

Through field measurement, it is found that the angle of damage boundary of working face 22,407 is 46°, and the angle of break is 70°. Compared with the angular parameters under general conditions, the corresponding angular parameters under high-strength mining conditions are small and the influence range is large.

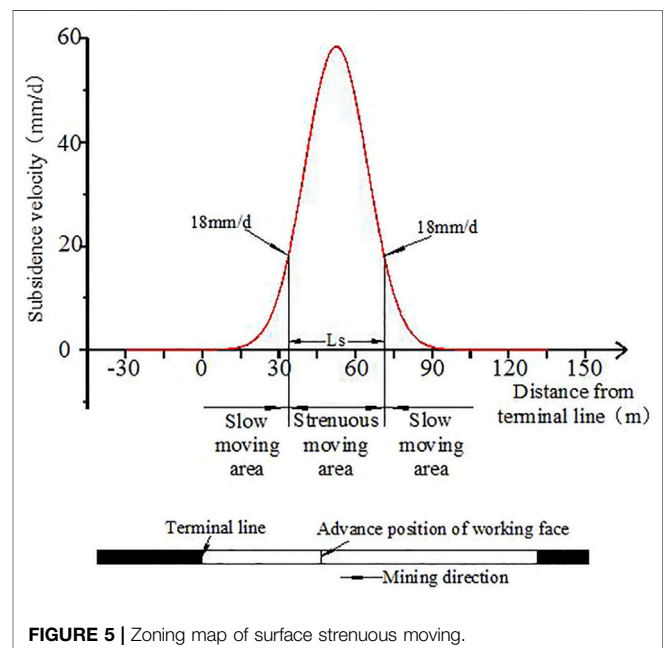


FIGURE 5 | Zoning map of surface strenuous moving.

TABLE 3 | Width of strenuous moving area.

	Width of strenuous moving area/m	Mining depth/m	Ratio of the strenuous moving area width to mining depth
2014-01-06	197	130	1.52
2014-01-08	205	130	1.58
2014-01-10	203	130	1.56
Average	201.7	130	1.55

TABLE 4 | Location of strenuous moving area.

Date	Distance between the advanced position of the working face and the left boundary of the strenuous moving area/L (m)	Width of strenuous moving area/L _s (m)	L/L _s
2014-01-06	40	191	0.209
2014-01-08	38	198	0.192
2014-01-10	38	202	0.188
Average	38.67	197	0.196

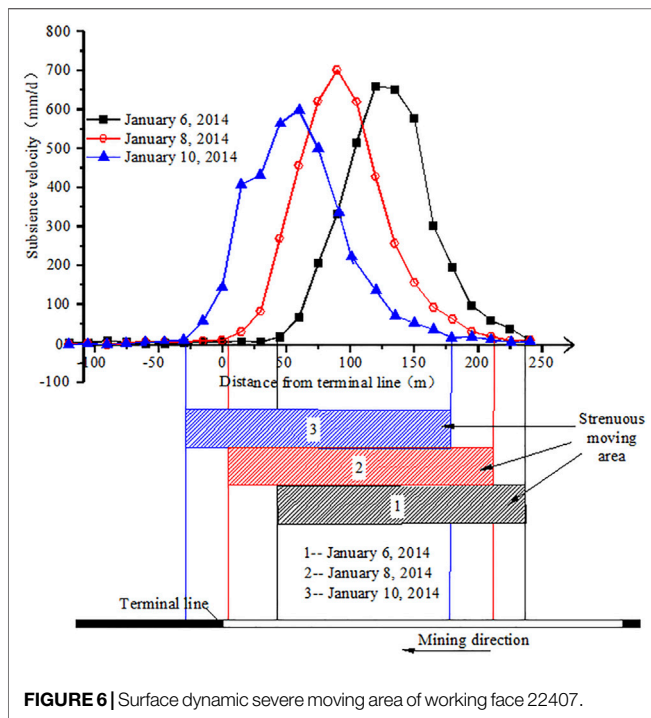


FIGURE 6 | Surface dynamic severe moving area of working face 22407.

4.2 Surface Damage Degree

The damage degree of the ground surface above the gob can be reflected by the magnitude of surface subsidence velocity. The surface subsidence velocity can be calculated by the following formula.

$$v_n = \frac{w_{i+1} - w_i}{t} \tag{4}$$

Where v_n is the subsidence velocity of point n ; w_{i+1} , w_i is the subsidence value of point n measured at $i + 1$ and i times, mm; and t is the interval between two measurements, d.

The maximum subsidence velocity of working face 22,407 is 700 mm/d, so the surface has undergone strenuous movement and violent deformation during the mining process under the condition of high-strength mining. To analyze the dynamic distribution laws of ground surface severe damage, we evaluated two aspects: the temporal and spatial distribution

characteristics of severe surface damage and the dynamic distribution laws of surface cracks.

4.2.1 Temporal Distribution of Surface Single Point Severe Damage

The surface point in the subsidence trough experiences the process from when it begins to move to the end of movement. The movement process of a surface point can be described by the subsidence velocity. The whole movement duration, according to the subsidence velocity, can be divided into three periods: initial period, active period, and weakening period (He et al., 1991; Peng, 1992; National Bureau of Coal Industry, 2017).

Initial period. From the beginning of the movement of the surface to the time when subsidence velocity reaches 1.67 mm/d or 50 mm/month.

Active period. Time interval when subsidence velocity is greater than 1.67 mm/d.

Weakening period. From the time when the movement of the surface decreases to 1.67 mm/d to the time when subsidence ends.

During these three periods, the surface points in the active period had the largest subsidence velocity and suffered the most damage. The longer the active period lasts, the more severe the damage to the surface points. The movement duration of working face 22,407 is shown in **Table 2**.

As can be seen from **Table 2**, the whole movement duration was 359 days, and the initial period, active period, and weakening period accounted for 2.5, 41.8, and 55.7% of the whole movement duration, respectively. The initial period was very short. The surface point entered the active period soon after it was affected by mining activities. The duration of the active period and weakening period was close to half of the whole movement duration. Compared with the traditional law (He et al., 1991; Peng, 1992; National Bureau of Coal Industry, 2017), it can be seen that under high-strength mining conditions, the active period was longer, and the severe damage to the surface point was more serious.

4.2.2 Spatial Distribution Law of Severe Surface Damage

At a certain time, the subsidence velocity differed for each point on the major section of the subsidence trough. According to the subsidence velocity, its strenuous movement degree can be

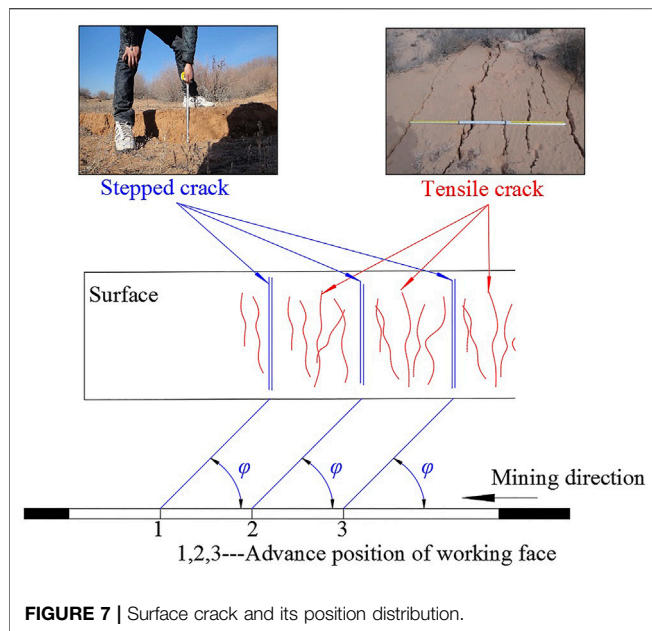


FIGURE 7 | Surface crack and its position distribution.

described by partition. A subsidence velocity of 18 mm/d was given as the critical value to define level IV damage to buildings. This paper also uses it to divide the dynamic subsidence trough into two zones (Figure 5).

Slow moving area: the surface subsidence velocity in this area is not greater than 18 mm/d; Strenuous moving area: the surface subsidence velocity in this area is larger than 18 mm/d.

When the face advances a sufficient distance, the width of strenuous moving area reaches its maximum possible value. The field-measured width of the strenuous moving area is shown in Table 3.

It can be seen from the above table that the strenuous moving area width was approximately 1.55 times the mining depth. That is, under high-strength mining conditions, the scope of the ground surface point moved violently and severe damages were generally large. The development of the strenuous moving area as the face advanced is shown in Figure 6.

The distance between the advanced position of the working face and the left boundary of the strenuous moving area under various advance positions of the working face measured in the Halagou coal mine are shown in Table 4.

From Table 3, the distance between the advanced position of the working face and the left boundary of the strenuous moving area for all three periods were equal to 1/5 of the strenuous moving area width. That is, the advanced position of working face was located at the left 1/5 of the strenuous moving area width.

In summary, under high-strength mining conditions, the time duration of severe damage to the surface points was relatively long, and the area where the surface was severely damaged was relatively wide. The severely damaged area was a dynamic area, which continuously moved forward as the working face advanced.

4.2.3 Surface Dynamic Crack and Its Development Rules

The ratio of mining depth to mining thickness of the high-strength mining working face was small and the dynamic crack was fully developed. The dynamic crack mainly had tensile cracks and stepped cracks as shown in Figure 7. The development of tensile crack had high density and small width. In addition, a stepped crack appeared in cycles.

The development of dynamic crack has the following characteristics:

- 1) A stepped crack lags behind the advanced position of working faces.

The overburden layer failure is developed along the direction of the bedrock fracture angle in the bedrock and along the similar vertical direction in the loose layer. The failure directly reaches to the surface and forms a stepped crack. A stepped crack lags behind the advanced position of the working face. The lag distance is called the lag distance of the stepped crack (Eq. 5), the corresponding angle is called the lag angle of the stepped crack (Eq. 6).

$$L_t = H_j \times \cot \gamma \quad (5)$$

$$\varphi = \arctan\left(\frac{L_t}{H_0}\right) \quad (6)$$

Where L_t is the lag distance of the stepped crack (m), φ is the lag angle of the stepped crack ($^\circ$), H_j is the thickness of bedrock (m), H_0 is the average mining depth (m), and γ is the bedrock fracture angle ($^\circ$).

A bedrock fracture angle of 52–57 $^\circ$ at the side of the working face was measured (Yan et al., 2018). An average angle value of 55 $^\circ$ was used as the bedrock fracture angle value. According to Eqs 2, 3, the lag distance of the stepped crack is 62.3 m and the lag angle of the stepped crack is 64.6 $^\circ$.

The field-measured lag distance of the stepped crack under various advanced positions of the working face are shown in Table 5. It can be seen from Table 5 that the calculation results are basically consistent with the field measurement results.

- 2) Stepped crack spacing and periodic weighting interval fairly.

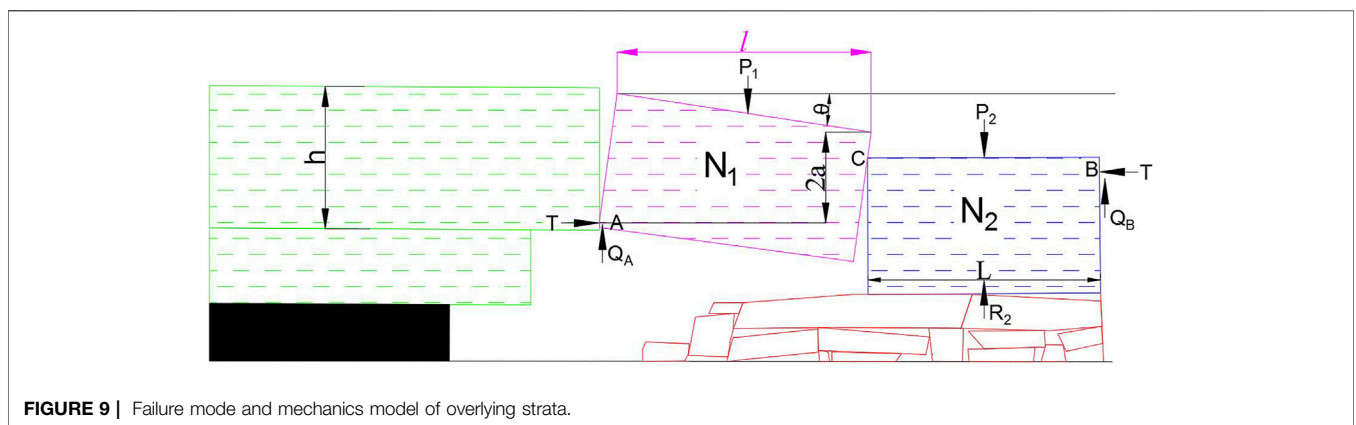
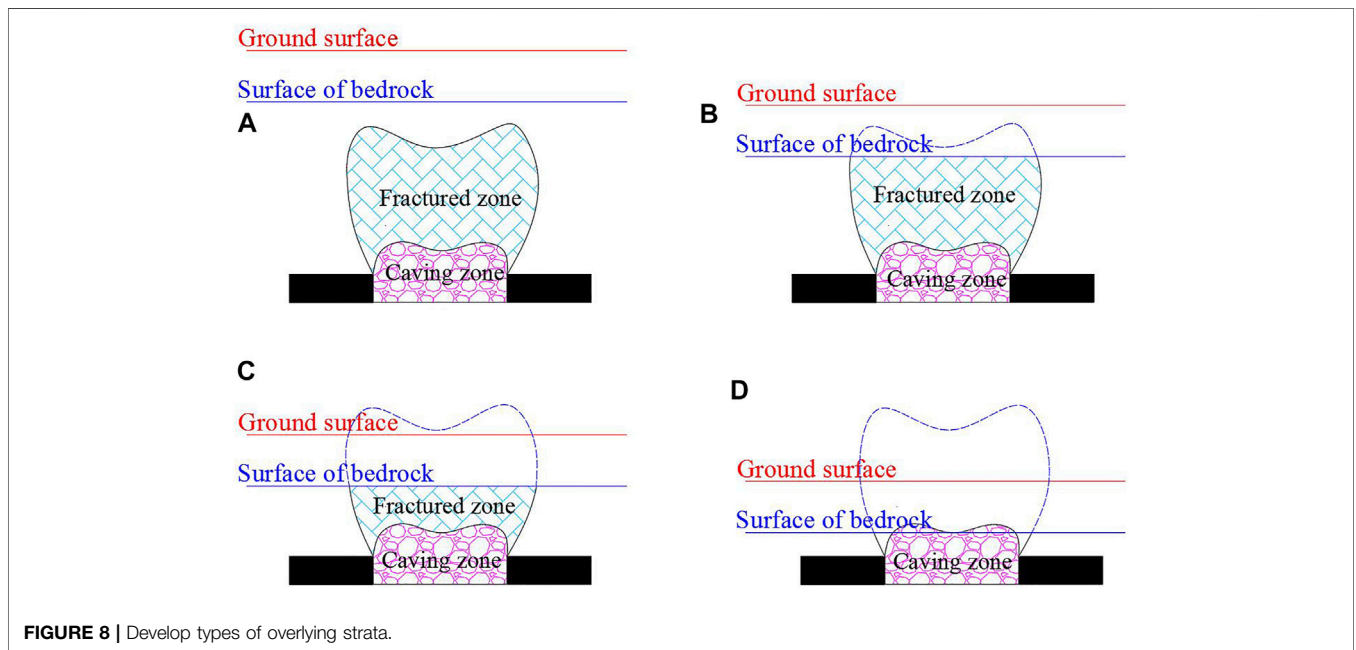
The measured spacing between stepped cracks is 8–11 m along the advance direction of the working face. The periodic weighting interval is 10 m, which is basically the same as the former.

5 DISCUSSION

In the vertical direction, under the condition of general geological mining, after rock strata movement, the overlying strata can be divided into three different mining influence areas: caving zone, fractured zone, and sagging zone. Because the caving zone and fractured zone easily conduct water, they are jointly called the water conducting fractured

TABLE 5 | Relative position of the stepped crack and the working face.

Date	Horizontal distance between the working face and terminal line/m	Horizontal distance between the outside stepped crack and terminal line/m	Horizontal distance between the outside stepped crack and working face/m
6 January 2014	77–94	146	52–69
8 January 2014	40–60	117	57–77
10 January 2014	3–19	78	59–75



zone. However, under special geological and mining conditions, the movement law of overlying strata is different, and the three mining influence zones in overburden strata do not exist at the same time. Which can be summarized as four types, as shown in **Figure 8**.

Type one: The “three zones” of overlying rock are fully developed. The caving zone, fractured zone, and sagging zone exist at the same time (**Figure 8A**).

Type two: The fracture zones directly reach the top surface of the bedrock, but do not reach the ground surface (**Figure 8B**).

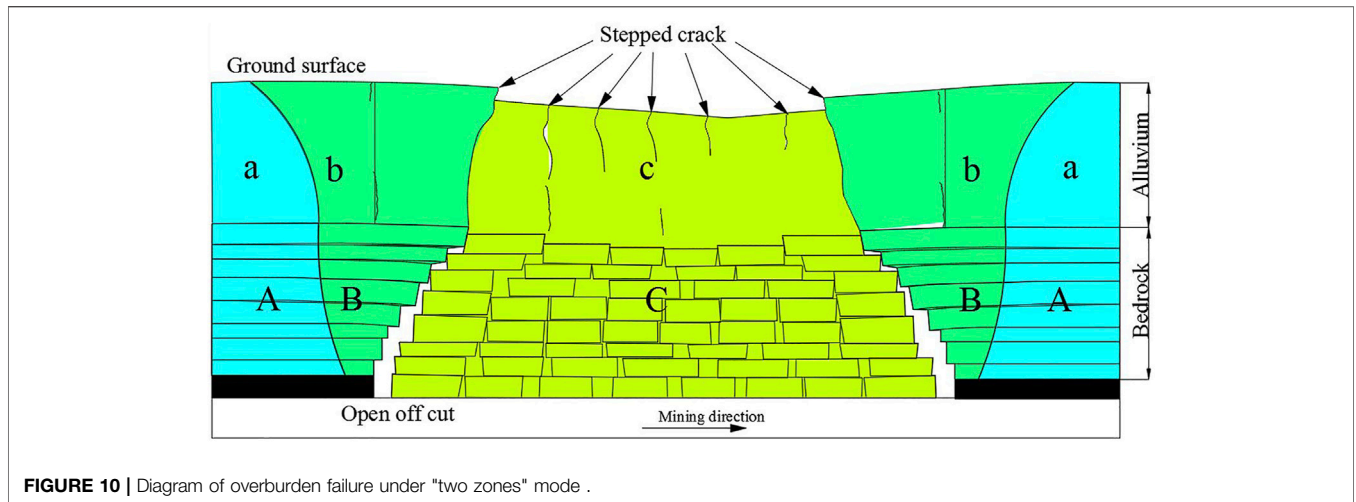


FIGURE 10 | Diagram of overburden failure under "two zones" mode .

Type three: The fracture zone directly reaches the ground surface (Figure 8C).

Type four: The caving zone directly reaches the top surface of bedrock (Figure 8D).

Under high-strength mining, the calculation formula of the height of caving zone and fracture zone is as follows (Yan et al., 2018).

$$H_c = (6.94M - 17.3) \pm 4.7 \quad (7)$$

$$H_f = (2.62M + 53.77) \pm 8.7 \quad (8)$$

Where H_c is the height of the caving zone; H_f is the height of the fracture zone; and M is the mining thickness.

Through calculation, it was found that the fracture zone height of working face 22,407 was greater than the bedrock thickness. The fractured zone directly reached the surface of bedrock. Therefore, the type of overlying strata movement of the working face conformed to type two. That is to say, the type of overlying strata movement of high-strength mining was the "two zones" mode.

Under the "two zones" mode, the migration of the roof is shown in Figure 9.

According to the moment equilibrium, Formulas 9–12 can be derived.

$$Q_A + Q_B = P_1 \quad (9)$$

$$T = \frac{lP_1}{2(h - a - w)} = \frac{P_1}{i - 2 \sin \theta_{\max} + \sin \theta} \quad (10)$$

$$Q_B = T \sin \theta_2 \quad (11)$$

$$a = 0.5(h - l \sin \theta) \quad (12)$$

Where Q is the shear force; P is the suffered load; T is the horizontal thrust; l is the length of rock block; h is the height of rock block; θ is the rotation angle of rock block; and i is the rock fragmental size, $i = l/h$.

Since θ_2 is very small, Q_B can be ignored, so $Q_A = P_1$. According to a previous study (Qian et al., 2012), the maximum value of θ in this area is 8–12°, i is greater than 1, and the tangent value of the friction angle is 0.5. When these

values are brought into the above formula, the following relationship can be obtained:

$$i - 2 \sin \theta_{\max} + \sin \theta > 0.584 \quad (13)$$

Therefore, the relationship between the shear force and friction force of the arch foot is calculated as follows.

$$T \tan \varphi = \frac{P_1}{i - 2 \sin \theta_{\max} + \sin \theta} < \frac{0.5P_1}{0.584} < P_1 = Q_A \quad (14)$$

It can be seen that the sliding instability easily occurs in the "two zones" mode. The sliding instability of the roof can easily lead to the stepped subsidence of strata and induce the overburden to break in full thickness. As seen in Figure 10, because the loose layer is prone to shear failure, the stepped subsidence of strata easily leads to the formation of stepped cracks on the ground surface.

Besides, the loose layer above working face 22,407 is thick, up to 55 m. And the cohesion between particles in the loose layer such as aeolian sand is small. This will lead to the following two situations.

- 1) The thick loose layer is equivalent to softening of the rock stratum, which increases the influence range and degree of surface mining.
- 2) Due to the weak anti-disturbance ability of the loose layer, the ground surface will be seriously damaged by underground high-strength mining, and it is easy for many small irregular tension cracks to appear on the ground surface between stepped cracks (Figure 7).

6 CONCLUSION

Through analysis of field-measured data, the characteristics of severe surface damage induced by high-strength mining were summarized. The main conclusions are as follows:

- 1) Severe surface damage lasts for a long time and has a wide range. The duration of the active period is close to half of the whole movement duration. The width of the strenuous moving area is equal to 1.55 times the mining depth. The advanced position of the working face is located at the left 1/5 of the strenuous moving area width. The strenuous moving area is a dynamic area, which continuously moves forward as the working face advances.
- 2) The dynamic crack types of surface and their periodic distribution laws induced by high-strength mining are summarized. The development of tensile cracks has high density and small width. In addition, stepped cracks appear in cycles, and the step crack spacing and the periodic weighting interval is consistent. The surface dynamic tensile cracks reflect the surface tension process between the two roof breakages.
- 3) The overburden strata failure in the “step beam” model and the strata move in the “two zones” mode. The sliding instability of the roof results in stepped subsidence of rock strata and further stepped cracks on the ground surface. In addition, rock strata are completely broken, resulting in severe surface damage.

DATA AVAILABILITY STATEMENT

The raw data supporting the conclusion of this article will be made available by the authors, without undue reservation.

REFERENCES

- Bai, E. H., Guo, W. B., Tan, Y., Huang, G. S., Guo, M. J., and Ma, Z. B. (2020). Roadway Backfill Mining with Super-high-water Material to Protect Surface Buildings: a Case Study. *Appl. Sci.* 10, 107. doi:10.3390/app10010107
- Bell, F. G., Stacey, T. R., and Genske, D. D. (2000). Mining Subsidence and its Effect on the Environment: Some Differing Examples. *Environ. Geol.* 40, 135–152. doi:10.1007/s002540000140
- Chen, C., Hu, Z. Q., Wang, J., and Jia, J. T. (2019). Dynamic Surface Subsidence Characteristics Due to Super-large Working Face in Fragile-Ecological Mining Areas: A Case Study in Shendong Coalfield, China. *Adv. Civ. Eng.* 2019, 1–16. doi:10.1155/2019/8658753
- Cui, X., Gao, Y., and Yuan, D. (2014). Sudden Surface Collapse Disasters Caused by Shallow Partial Mining in Datong Coalfield, China. *Nat. Hazards* 74, 911–929. doi:10.1007/s11069-014-1221-5
- Fan, G. W., Zhang, D. S., and Ma, L. Q. (2011). Overburden Movement and Fracture Distribution Induced by Longwall Mining of the Shallow Coal Seam in the Shendong Coalfield. *J. China Univ. Min. Tech.* 40, 196–201.
- Fan, L. M., Zhang, X. T., and Xiang, M. X. (2015). Characteristics of Ground Fissure Development in High-Intensity Mining Area of Shallow Seam in Yushenfu Coal Field. *J. China Coal Soc.* 40, 1442–1447. doi:10.13225/j.cnki.jccs.2014.1707
- He, G. Q., Yang, L., and Ling, G. D. (1991). *Mining Subsidence Theory*. Xuzhou, China: China University of Mining and Technology Press.
- Ju, J., and Xu, J. (2013). Structural Characteristics of Key Strata and Strata Behaviour of a Fully Mechanized Longwall Face with 7.0m Height Chocks. *Int. J. Rock Mech. Min. Sci.* 58, 46–54. doi:10.1016/j.ijrmms.2012.09.006
- Lian, X., Zhang, Y., Yuan, H., Wang, C., Guo, J., and Liu, J. (2020). Law of Movement of Discontinuous Deformation of Strata and Ground with a Thick Loess Layer and Thin Bedrock in Long Wall Mining. *Appl. Sci.* 10, 2874. doi:10.3390/app10082874
- Luo, Y., and Cheng, J. W. (2009). An Influence Function Method Based Subsidence Prediction Program for Longwall Mining Operations in Inclined Coal Seams. *Min. Sci. Tech.* 19, 0592–0598. doi:10.1016/s1674-5264(09)60110-1

AUTHOR CONTRIBUTIONS

Conceptualization, WY; methodology, JC; software, WY; validation, YT and JG; formal analysis, WY; investigation, SY; resources, YY; data curation, JG; writing—original draft preparation, WY; writing—review and editing, WY; visualization, JG; supervision, YT; project administration, JC; funding acquisition, JC. All authors have read and agreed to the published version of the manuscript.

FUNDING

This research was funded by the Open Fund of State Key Laboratory of Water Resource Protection and Utilization in Coal Mining (grant numbers WPUKFJ2019-20 and WPUKFJ2019-17), the Henan Scientific and Technological Projection (grant number 212102310012), the National Natural Science Foundation of China (grant numbers U21A20108 and 51974105), the Fundamental Research Funds for the Universities of Henan Province (grant number NSFRF200314), the Youth Backbone Teacher Support Program of Henan Polytechnic University (2019XQG-07), and Doctoral Fund Program of Henan Polytechnic University (B2017-07, B2019-03).

- Ma, L., Zhang, D., Sun, G., Cui, T., and Zhou, T. (2013). Thick Alluvium Full-Mechanized Caving Mining with Large Mining with Large Mining Height Face Roof Control Mechanism and Practice. *J. China Coal Soc.* 38, 199–203. doi:10.13225/j.cnki.jccs.2013.02.017
- National Bureau of Coal Industry (2017). *Pillars and Mining Regulation of Building, Water, Railway and Main Shaft and Tunnel*. Beijing, China: China Coal Industry Publishing House.
- Peng, S. S. (1992). *Surface Subsidence Engineering*. New York, USA: Society of Mining Engineers.
- Qian, M. G., Shi, P. W., and Xu, J. L. (2012). *Mining Pressure and Strata Control*. Xuzhou: China Uni Min Tech Pub, 374.
- Ramesh, P. S., and Ram, N. Y. (1995). Prediction of Subsidence Due to Coal Mining in Raniganj Coalfield, West Bengal, India. *Eng. Geol.* 39, 103–111. doi:10.1016/0013-7952(94)00062-7
- Ren, G., Whittaker, B. N., and Reddish, D. J. (1989). Mining Subsidence and Displacement Prediction Using Influence Function Methods for Steep Seams. *Min. Sci. Technol.* 8, 235–251. doi:10.1016/s0167-9031(89)90393-9
- Saha, S., Pattanayak, S. K., Sills, E. O., and Singha, A. K. (2011). Under-mining Health: Environmental Justice and Mining in India. *Health & Place* 17, 140–148. doi:10.1016/j.healthplace.2010.09.007
- Salmi, E. F., Nazem, M., and Karakus, M. (2017). The Effect of Rock Mass Gradual Deterioration on the Mechanism of Post-mining Subsidence over Shallow Abandoned Coal Mines. *Int. J. Rock Mech. Min. Sci.* 91, 59–71. doi:10.1016/j.ijrmms.2016.11.012
- Sasaoka, T., Takamoto, H., Shimada, H., Oya, J., Hamanaka, A., and Matsui, K. (2015). Surface Subsidence Due to Underground Mining Operation under Weak Geological Condition in Indonesia. *J. Rock Mech. Geotechnical Eng.* 7, 337–344. doi:10.1016/j.jrmge.2015.01.007
- Sinha, S., Bhattacharya, R. N., and Banerjee, R. (2007). Surface Iron Ore Mining in Eastern India and Local Level Sustainability. *Resour. Policy* 32, 57–68. doi:10.1016/j.resourpol.2007.06.001
- Suchowerska Iwanec, A. M., Carter, J. P., and Hambleton, J. P. (2016). Geomechanics of Subsidence above Single and Multi-Seam Coal Mining. *J. Rock Mech. Geotechnical Eng.* 8, 304–313. doi:10.1016/j.jrmge.2015.11.007

- Tang, F.-q. (2009). Research on Mechanism of Mountain Landslide Due to Underground Mining. *J. Coal Sci. Eng. China* 15, 351–354. doi:10.1007/s12404-009-0403-3
- Thongprapha, T., Fuenkajorn, K., and Daemen, J. J. K. (2015). Study of Surface Subsidence above an Underground Opening Using a Trap Door Apparatus. *Tunn. Undergr. Space Technol.* 46, 94–103. doi:10.1016/j.tust.2014.11.007
- Vervoort, A. (2016). Surface Movement above an Underground Coal Longwall Mine after Closure. *Nat. Hazards Earth Syst. Sci.* 16, 2107–2121. doi:10.5194/nhess-16-2107-2016
- Wang, J. Z., Kang, J. R., and Chang, Z. Q. (1999). The Mechanism Analysis on the Dissymmetry of the Surface Subsidence Basin. *J. China Coal Soc.* 24, 252–255.
- Yan, W., Chen, J., and Yan, Y. (2019). A New Model for Predicting Surface Mining Subsidence: the Improved Lognormal Function Model. *Geosci. J.* 23, 165–174. doi:10.1007/s12303-018-0008-1
- Yan, W., Dai, H., and Chen, J. (2018). Surface Crack and Sand Inrush Disaster Induced by High-Strength Mining: Example from the Shendong Coal Field, China. *Geosci. J.* 22, 347–357. doi:10.1007/s12303-017-0031-7
- Yu, B., Zhao, J., Kuang, T., and Meng, X. (2015). *In Situ* investigations into Overburden Failures of a Super-thick Coal Seam for Longwall Top Coal Caving. *Int. J. Rock Mech. Min. Sci.* 78, 155–162. doi:10.1016/j.ijrmmms.2015.05.009
- Zhang, J., and Chong, L. (2012). The Discussion of the Surface and Building Deformation in the Coal Mining Subsidence Area. *Shanxi Archit.* 38 (09), 83–84. doi:10.13719/j.cnki.cn14-1279/tu.2012.09.012

Conflict of Interest: The authors declare that the research was conducted in the absence of any commercial or financial relationships that could be construed as a potential conflict of interest.

Publisher's Note: All claims expressed in this article are solely those of the authors and do not necessarily represent those of their affiliated organizations, or those of the publisher, the editors and the reviewers. Any product that may be evaluated in this article, or claim that may be made by its manufacturer, is not guaranteed or endorsed by the publisher.

Copyright © 2022 Yan, Guo, Chen, Tan, Yan and Yan. This is an open-access article distributed under the terms of the Creative Commons Attribution License (CC BY). The use, distribution or reproduction in other forums is permitted, provided the original author(s) and the copyright owner(s) are credited and that the original publication in this journal is cited, in accordance with accepted academic practice. No use, distribution or reproduction is permitted which does not comply with these terms.